



Analysis of the performance of driver MOX fuel in the MYRRHA reactor under Beam Power Jump transient irradiation conditions

A. Magni, M. Di Gennaro, E. Guizzardi¹, D. Pizzocri, G. Zullo, L. Luzzi*

Politecnico di Milano, Department of Energy, Nuclear Engineering Division, via La Masa 34, 20156 Milano, Italy

ARTICLE INFO

Keywords:

MYRRHA reactor
MOX fuel
Fuel pin performance
TRANSURANUS
Design and safety analysis

ABSTRACT

This work focuses on the performance analysis of driver fuel pins under transient irradiation conditions in the MYRRHA reactor, which must be considered besides the normal operation towards the design optimization and licensing of the facility. The considered transient scenario is a Beam Power Jump (BPJ) caused by a trip of the MYRRHA accelerator coupled to the sub-critical reactor core. Based on the outcomes of the analysis of the nominal MYRRHA irradiation - NED 386 (2022) 111581, the impact of this over-power scenario on the pin response is investigated both at the beginning and at the end of irradiation as the most critical moments for the fuel maximum temperature and for the potential fuel-cladding mechanical interaction, respectively. The simulation results are achieved with the TRANSURANUS fuel performance code equipped with advanced models for thermal-mechanical properties of U-Pu mixed-oxide (MOX) fuels, for inert gas behaviour and for the specific mechanical response of DIN 1.4970 cladding. The comparison with design limit criteria adopted highlights the safety of the MYRRHA fuel pins under irradiation, complying with satisfactory margins even considering the occurrence of BPJ transients.

1. Introduction

The MYRRHA facility (Multi-purpose hYbrid Research Reactor for High-tech Applications) (Ait Abderrahim et al., 2020; Ait Abderrahim et al., 2019) is under design and construction at the Belgian nuclear research centre SCK CEN as a flexible irradiation facility for research and development purposes (MYRRHA Consortium, 2022). It is part of the ESNII (European Sustainable Nuclear Industrial Initiative) roadmap for the development of Generation IV nuclear reactors (Locatelli et al., 2013; GIF (Generation IV International Forum), 2018, 2020) and it is conceived as an experimental accelerator driven system (ADS) coupled to a fast reactor cooled by lead-bismuth eutectic (LBE). The aims of the facility are to demonstrate the ADS concept itself at an industrial level and to study the technological feasibility and efficiency of transmuting minor actinides and long-lived fission products under fast neutron irradiation (Ait Abderrahim et al., 2020). This matches the R&D needs and expectations related to fast reactors of Generation IV (SNETP, 2020). Further objectives of MYRRHA consist in allowing the investigation of the behaviour under irradiation of materials for Gen-IV and

fusion reactors (enabled by the high-energy shoulder offered by the MYRRHA spectrum (Romero et al., 2017, 2019), and in producing radioisotopes for medical and industrial applications.

The design optimization and safety analyses phases, fundamental towards the licensing of the facility, include the consideration of transient scenarios besides the normal operation conditions. Indeed, the compliance with safety requirements must be guaranteed in any scenario of reactor operation. Hence, besides the irradiation conditions designed for the MYRRHA normal operation (composed by 12 power cycles and already analysed in Magni et al. (2022)), Beam Power Jump (BPJ) transients are considered in this work. These fast over-power ramps, of concern for the MYRRHA sub-critical core configuration coupled to an external accelerator, could occur at any moment during the normal reactor operation but are herein investigated at beginning-of-life conditions (cycle 1) and at end-of-irradiation conditions (cycle 12). These scenarios are deemed as the most critical for the fuel maximum temperature and for the pellet-cladding mechanical interaction under eventual fuel-cladding gap closure conditions, respectively, based on the results of MYRRHA normal operation already obtained

* Corresponding author.

E-mail address: lelio.luzzi@polimi.it (L. Luzzi).

¹ Current address: Newcleo, via Giuseppe Galliano 27, 10129 Torino, Italy.

with TRANSURANUS and previously published in Magni et al. (2022). Hence, they require dedicated evaluations to ensure the safe operation of MYRRHA during any irradiation condition. In fact, the ultimate goal of this activity is to evaluate the overall safety under irradiation, even under operational transients, of the MYRRHA pins by verifying the compliance with the current MYRRHA design limits. The main ones concern an upper limit for the fuel maximum temperature, in order to avoid failures related to fuel melting, and an allowed maximum cladding plasticity, to ensure cladding integrity under the potential joint action of gap pressure and eventual gap closure.

The pin performance assessment under transient conditions for the MYRRHA reactor is presented in this work, referring to the pin and core specifications associated to the MYRRHA design "Revision 1.6" (De Bruyn et al., 2016; Magni et al., 2022). The driver fuel to be employed in MYRRHA for the normal reactor operation consists of U-Pu mixed-oxides (MOX), clad within DIN 1.4970, a stainless-steel of the 15-15Ti family (Magni et al., 2022). The thermal-mechanical behaviour of the MYRRHA pins is simulated by means of the TRANSURANUS fuel performance code (Lassmann, 1992; Magni et al., 2021). An upgraded version of the code is applied here, equipped with recent models developed for MOX thermal properties (thermal conductivity, melting temperature), MOX mechanical properties (thermal expansion, Young's modulus), and for the mechanistic treatment of fission gas behaviour and release from MOX fuels. This TRANSURANUS version corresponds to that reported and assessed against the SUPERFACT-1 fast reactor irradiation experiment in Luzzi et al. (2023). Besides the advanced fuel modelling, specific correlations for the mechanical behaviour under irradiation of the DIN 1.4970 cladding are applied, already used for the analysis of the MYRRHA normal operation (Magni et al., 2022).

Moreover, as in Magni et al. (2022), the performance under irradiation of the MYRRHA hottest pin is analysed in this work under the same conservative assumption of this pin being in the hottest position during each of the 12 irradiation cycles designed for the normal reactor operation.² This approach guarantees that cautious conclusions are drawn from the analyses, holding for every pin under irradiation in the MYRRHA core since the worst possible conditions and scenarios associated to the current reactor design are here taken into account.

The paper is structured as follows. Section 2 outlines the BPJ scenarios analysed and the safety criteria adopted for the transient irradiation of MYRRHA pins. The set-up and results yielded by the pin performance simulations are presented in Section 3, while the assessment of the pin safety against the design limits is provided in Section 4. Conclusions are drawn in Section 5, complemented by perspectives beyond this work.

2. Description of the MYRRHA irradiation scenarios

MYRRHA is designed as a pool-type fast reactor cooled by lead-bismuth eutectic (LBE), able to operate both in critical and sub-critical mode (i.e., as an ADS) (Ait Abderrahim et al., 2012). In the ADS configuration, the MYRRHA sub-critical core is coupled to a proton accelerator delivering its beam to a liquid LBE spallation target localized in a dedicated assembly at the core centre. The optimal solution for the ADS design and performances turned out to be a 600 MeV linear accelerator (LINAC) with an average proton beam current up to 4 mA (De Bruyn et al., 2015; Engelen et al., 2015). For details about the design of the MYRRHA LBE-cooled reactor, the reader is referred to (Fernandez et al., 2017; Toti et al., 2018). The reference for this work is the MYRRHA "Revision 1.6" design, sub-critical core configuration, already outlined and analysed (normal operating conditions) by the same authors (Magni et al., 2022).

² It is called *hypothetical* hottest pin in Magni et al. (2022), identified on purpose for a conservative evaluation of the pin performance under irradiation since experiencing the worst irradiation conditions in terms of power, neutron flux, temperature.

As far as the selection of pin materials is concerned, the employment in MYRRHA of mature technologies in terms of readiness level and less demanding technologies from the research and development point of view is favoured (Ait Abderrahim et al., 2005). Following this approach, an austenitic, 15-15Ti stainless-steel (specifically, the DIN 1.4970 alloy annealed and cold worked) has been selected as pin cladding. The U-Pu MOX driver fuel contains 30% of plutonium and 70% of natural uranium, a composition already considered in Magni et al. (2022).

The designed MYRRHA operating schedule consists of 90 Effective Full Power Days (EFPD) and the nominal driver fuel irradiation is composed by 12 cycles (Van Den Eynde et al., 2015). After each irradiation cycle, a core reconfiguration is foreseen: batches composed by six fuel assemblies are shuffled towards outer regions of the MYRRHA core, while fresh fuel is added close to the central spallation target (in the first ring of the core (Magni et al., 2022)), in order to compensate the core reactivity loss. In this way, the final fuel burnup at the end of the driver irradiation for each fuel element is homogenized and is expected to be around 70 GWd/t_{HM}, both in critical and sub-critical core configurations.

2.1. Beam Power Jump transient

The over-power transient scenario considered in this work is specific for the ADS configuration of MYRRHA and consists of a Beam Power Jump (Magni et al., 2022). The initiating event for the BPJ transient is an accelerator over-current, i.e., a sudden increase by (maximum) 70% of the proton source while the accelerator is working in nominal conditions (beam intensity: 4 mA, beam energy: 600 MeV, reactor core power: 70 MW). The accelerator control system reacts to the beam trip, increasing by 70% the feeding power in order to keep the beam energy constant at the target operational value. The maximum feeding power is limited to 170% of the nominal value by the fault tolerance scheme implemented in the high-energy section of the accelerator. Consequently, the power of the MYRRHA ADS core also increases by 70% due to the proportionality between the proton current and the core power (neutron flux). Neglecting conservatively the effect of delayed neutrons on the core power evolution, it is here assumed that the reactor power reaches the limit value of 170% of the operating power in 1 ms by effect of the BPJ, without affecting the peak factors for the axial pin power profile. The high neutron flux signal prolonging for more than 3 seconds triggers the accelerator shut-off, for which a scram time of 3 seconds is conservatively assumed. In fact, a tolerance of 3 seconds is designed for the duration of the MYRRHA accelerator beam trips, while shorter beam trips are allowed without limitations in terms of frequency of occurrence. Nevertheless, in terms of extent of the fault, just power oscillations lower than +70% of the nominal power are accepted. A sketch of the BPJ trips accounted for in this work is reported in Fig. 1, with reference to the peak power node of the hottest pin during each MYRRHA irradiation cycle.

The BPJ scenario can occur at any instant of time during the MYRRHA normal operation composed by 12 irradiation cycles. Based on the performance results of MOX driver fuel pins during the nominal irradiation history (Magni et al., 2022), two BPJ scenarios of major interest in terms of critical fuel pin performance are identified. The first one corresponds to a BPJ occurring at the end of the first cycle (BPJ1), when the fuel is at beginning-of-life conditions in the first ring of the MYRRHA core and the fuel pin is irradiated at the highest linear power, providing the highest fuel (and cladding) temperatures. Consequently, the smallest margin to fuel melting is expected from this transient scenario. The second one is the BPJ occurring at the end of the 12th cycle (BPJ12, before reactor shutdown and final batch discharge from the core), representative for end-of-irradiation and high burnup conditions when the fuel-cladding gap width is reduced and the effects of fuel-cladding mechanical interactions are potentially the strongest if gap closure is reached. Hence, BPJ12 corresponds to significant cladding damage conditions when potentially cladding plasticity can be reached.

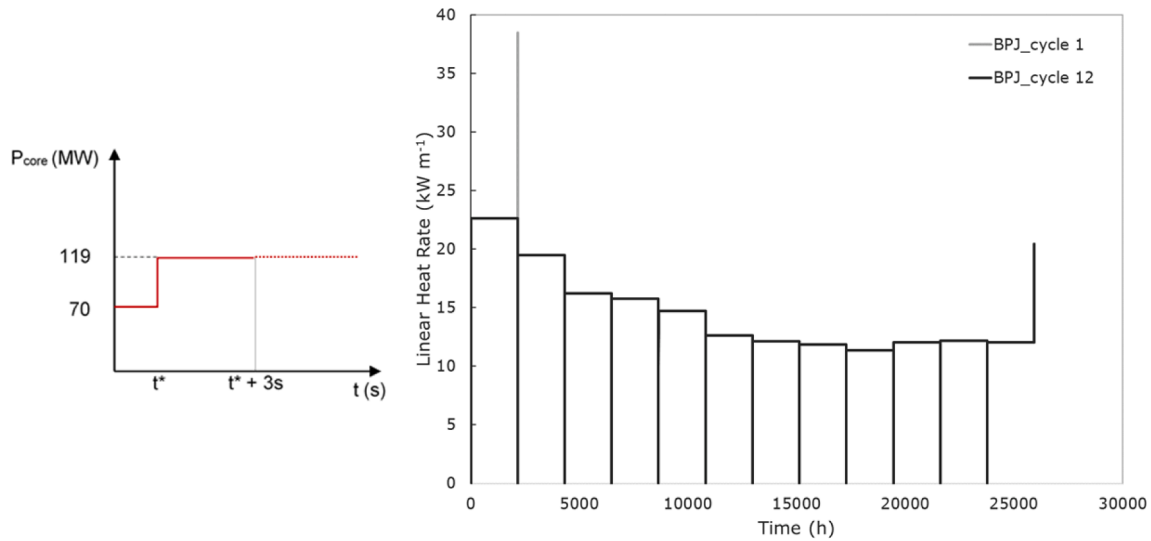


Fig. 1. Sketch of the MYRRHA power excursion in a BPJ scenario (Magni et al., 2022) (left) and linear power histories of the MYRRHA hottest pin (peak power node values) inclusive of the BPJ transients occurring at the end of cycle 1 and at the end of cycle 12 (right).

2.2. Design limit criteria

The main concern for the pin integrity and safety during over-power transient scenarios (as the BPJ of interest for MYRRHA) is represented by phenomena connected with fuel melting or by cladding mechanical failure (enhanced by pellet-cladding mechanical interaction). Hence, the following criteria are considered here for the assessment of the safety under transient irradiation of the thermal-mechanical behaviour of MYRRHA pins, in line with those already identified in Magni et al. (2022), Magni et al. (2022):

- Maximum fuel temperature conservatively limited at 2600 °C to prevent failures caused by fuel melting.
- Cladding plastic strain allowed up to 0.5% to guarantee structural integrity.

The pin performance under normal operating conditions must also comply with appropriate design limits (Magni et al., 2022), in particular maximum cladding temperatures both at the outer and inner surfaces, to prevent coolant-side corrosion and fuel-side corrosion in case of gap closure, respectively. The assessment of these criteria is already demonstrated in Magni et al. (2022), while they are not relevant in the present analysis due to the fast dynamics of the BPJ scenarios, shorter than the time scales on which corrosion acts and hence limiting in any case eventual corrosion-related issues.

The objective of the pin performance analysis performed in this work is to conservatively assess any pin failure potentially caused by a BPJ occurring in the MYRRHA sub-critical core. This is achieved by means of a combination of approaches, i.e., by considering the hottest MYRRHA pin during each irradiation cycle, by analysing the worst BPJ transients (i.e., occurring at the most critical irradiation cycles) in terms of the main safety criteria and by accounting for conservative design limit values. This kind of analysis allows providing the most careful code predictions in terms of pin safety even under transient operation. In particular, the selected design limit for the fuel melting is deliberately lower than the actual melting temperature of the MYRRHA fuel, considering its composition and irradiation conditions (Magni et al., 2022, 2020).

3. Simulation results

3.1. Simulation set-up

The present analysis of the MYRRHA pin performance under BPJ transient conditions is performed by applying the TRANSURANUS code (Lassmann, 1992; Magni et al., 2021), in its version v1m4j22 equipped with recent and upgraded models for the properties / behaviour of MOX fuels and for the mechanical response of the MYRRHA cladding.³ Specifically:

- The models employed for the MOX fuel properties include recently developed, physically-grounded and comprehensive correlations for thermal properties (thermal conductivity and melting temperature) (Magni et al., 2020, 2021), together with advanced correlations for mechanical properties (thermal expansion and Young's modulus) (Lemehov, 2020). These models have been already integrally assessed against fast reactor irradiation experiments (Luzzi et al., 2023) and applied to the fuel design for the sodium-cooled Generation IV concept (Magni et al., 2022).
- The coupling of TRANSURANUS with the SCIENTIX code (Pizzocri et al., 2020; Pizzocri et al., 2021; Van Uffelen et al., 2020), used as inert gas behaviour module, is herein applied for a physics-based description of fission gas behaviour in MOX fuel pellets, providing a coherent description of fuel gaseous swelling and fission gas release (FGR) in the fuel-cladding gap.
- Advanced models of thermal and irradiation-induced creep strain, thermal creep time-to-rupture and void swelling of the specific MYRRHA cladding material (DIN 1.4970), developed / reviewed in Magni et al. (2022), are also used for the present analysis.

³ The performance analysis of MYRRHA driver fuel pins under normal operation, published in Magni et al. (2022), was already achieved by means of the TRANSURANUS fuel performance code (version v1m1j20) employing the code recommended models for MOX fuel properties and fission gas behaviour. In particular, as for fission gas behaviour under fast reactor conditions, version v1m1j20 includes a treatment of the intra- and inter-granular dynamics of fission gases, but relies on a correlation-based approach for fission gas release and fuel gaseous swelling.

Hence, the model choices correspond to those adopted in Luzzi et al. (2023) for what concerns the fuel side, complemented by dedicated cladding property models, for the most appropriate simulation of the thermal–mechanical performance of MYRRHA pins. For what concerns all the remaining pin properties and phenomena, the best-estimate TRANSURANUS models for the MYRRHA fuel, cladding and coolant materials are used, i.e., those currently recommended inside the code to describe the behaviour under irradiation of fast reactor MOX fuels, 15-15Ti cladding steel (European Commission, 2022; Luzzi et al., 2014) and liquid LBE coolant (OECD/NEA, 2015). This corresponds to the approach already followed for the analysis of the MYRRHA normal operation (Magni et al., 2022), where a model for the corrosion of the outer cladding by the flowing LBE was not considered, although it impacts both the thermal performance of the pin (including the fuel temperatures) and the mechanical performance (and structural integrity) of the cladding. The formation and growth of an outer oxide layer on the cladding can be relevant during normal operation, but this has been already excluded for MYRRHA in Magni et al. (2022) by comparison with the design limit preventing corrosion issues. Moreover, corrosion acts on longer time scales compared to the fast BPJ transients, hence it is not relevant during the over-power transient scenarios addressed in this work. The modelling of corrosion effects requires dedicated experimental knowledge as a support, but it is challenging to obtain these data due to e.g., the specificities of the cladding-coolant material couple and the wide spectrum of possible test conditions in terms of temperature and oxygen content in the liquid LBE. For these reasons, and since a specific model for the corrosion of DIN 1.4970 cladding by LBE coolant is not currently available in the TRANSURANUS fuel performance code, the potential oxidation of the outer surface of the MYRRHA cladding is still not considered by the present simulations but it is recalled as a generally important modelling advancement for the assessment of liquid metal-cooled systems.

3.2. BPJ at the beginning of irradiation (cycle 1)

The most relevant impact of a BPJ occurring at cycle 1 (when the assembly is in the first ring of the MYRRHA core, at the highest MYRRHA linear power $\sim 22.7 \text{ kW m}^{-1}$) is the sudden increase of the fuel, cladding and coolant temperatures, as shown in Figs. 2 and 3. The bottom part of Fig. 2 provides a zoom on the step-wise dynamics of the temperature evolutions during the fast BPJ ramp, followed by the new temperature levels associated to the highest linear power $\sim 38.7 \text{ kW m}^{-1}$ reached with the BPJ1. These increased fuel and cladding temperatures are sustained for 3 s before automatic accelerator shut-off and reactor scram.

The TRANSURANUS calculation yields a fuel central temperature at the axial peak power node of $\sim 2455^\circ\text{C}$ in case of a BPJ occurring at the end of the first cycle, i.e., when the fuel central temperature during normal operation is the highest (Magni et al., 2022) (Fig. 2 – top left). That is the overall highest temperature potentially reached by the driver MOX fuel during the MYRRHA reactor operation, according to the TRANSURANUS simulation. It is sensibly impacted by the large temperature jump caused by the BPJ1, corresponding to $\sim 930^\circ\text{C}$.

Compared to the result presented in Magni et al. (2022), obtained with a previous TRANSURANUS code version (v1m1j20) equipped just with the DIN 1.4970 models, the results presented here correspond to lower fuel temperatures during the first cycle of MYRRHA normal operation, i.e., $\sim 1525^\circ\text{C}$ instead of 1680°C for the fuel central temperature at the end of the nominal irradiation cycle 1. This is related to the upgraded correlation for the MOX thermal conductivity (higher at low fuel burnup compared to the correlation by Schubert et al. (2004) employed in Magni et al. (2022) for the *reference* simulation case), the effect on the gap conductance of the novel correlation for the MOX thermal expansion (providing a slightly lower residual gap width during cycle 1), and to the physics-based treatment of fission gas behaviour and release obtained here via the SCIANTEX module coupled to

TRANSURANUS. A lower FGR during cycle 1, coherent with the intra- and inter-granular dynamics of gas in the fuel, degrades less the conductivity of the gas mixture in the gap at low fuel burnup levels. The impact of fission gas release on the pin performance during the entire driver fuel irradiation designed for MYRRHA is analysed in more detail in Section 3.3, dedicated to the BPJ12 occurring at high fuel burnup.

Fig. 3 shows the axial profiles of fuel central temperature (following the axial distribution of pin linear power) and residual fuel-cladding gap width before and after BPJ1. The radial gap width progressively reduces during cycle 1 from the as-fabricated size of $115 \mu\text{m}$ to $\sim 53 \mu\text{m}$ at the peak power node. At this axial location, the BPJ1 causes an additional reduction of the gap width down to $\sim 34 \mu\text{m}$ driven by the sudden thermal expansion of the fuel pellet. TRANSURANUS does not predict any gap closure by effect of BPJ1 and hence no fuel-cladding interaction occurs. Compared to the results of the standard code version (Magni et al., 2022), a slightly lower gap width is provided by the correlation for MOX thermal expansion applied here, which in turn contributes to lower fuel temperatures during the first irradiation cycle, as previously mentioned.

The cladding inner and outer temperatures, at the top of the fuel column where coolant and cladding are the hottest, jump from $\sim 450^\circ\text{C}$ and 434°C before the BPJ at the end of the first irradiation cycle to $\sim 595^\circ\text{C}$ and 568°C after the BPJ1, respectively (Fig. 4 in terms of axial profiles, coherent with the evolution in time shown by Fig. 2 - right). The coolant correspondingly jumps from $\sim 418^\circ\text{C}$ to $\sim 542^\circ\text{C}$. The fast increase of the cladding temperature during the BPJ1 transient causes a step-wise cladding radial deformation due to thermal expansion, besides the sudden thermal expansion of the fuel. Nevertheless, the total fuel deformation, inclusive of thermal creep and gaseous swelling (complementary to fission gas release), is higher than the cladding one mainly due to the higher temperature regime. This determines the dynamics of gap width reduction towards the end of the first irradiation cycle, where BPJ1 occurs.

3.3. BPJ at the end of irradiation (cycle 12)

Fig. 5 - left shows the TRANSURANUS results of fuel central temperature during the complete, 12-cycles irradiation history designed for the MYRRHA driver fuel. The increase of the fuel central temperature towards the end of irradiation is attributable to the decrease of the gap conductance determined by fission gas release (degrading the thermal conductivity of the gas mixture in the gap, Fig. 6 – right), besides the lowering of the fuel thermal conductivity with increasing burnup. The fuel temperature evolution is driven mostly by the effect of FGR in the fuel-cladding gap rather than by the gap width progressive reduction (Fig. 6 – left), especially from the fourth irradiation cycle on when the cumulated FGR becomes important. The occurrence of BPJ12 leads the fuel central temperature at the peak power node from $\sim 1635^\circ\text{C}$ to $\sim 2135^\circ\text{C}$. Both the temperature jump caused by BPJ12 and the maximum temperature reached are lower than the results yielded by the code simulation of BPJ1 (Section 3.2), since the linear power of normal operation at cycle 12 is $\sim 12 \text{ kW m}^{-1}$ instead of $\sim 22.7 \text{ kW m}^{-1}$ at cycle 1. The 12th irradiation cycle is indeed performed in the outer ring of the MYRRHA sub-critical core, the farthest location from the central core spallation channel. Consequently, the linear power reached after BPJ12 is just $\sim 20.5 \text{ kW m}^{-1}$. In terms of axial profile (Fig. 7), the fuel central temperature is still mostly determined by the axial linear power distribution, hence the highest temperature is predicted around the fuel mid-plane where the peak power node is located, despite the lowest residual width of the fuel-cladding gap.

Fig. 5 – left shows that the predicted fuel central temperature during normal operation is actually higher at mid-irradiation and towards the end of irradiation (from cycle 4 on) than at cycle 1, mainly due to two combined effects: a progressively lower gap conductance driven by an increasing fission gas release in the gap (Fig. 6 – right), and the degradation of the fuel thermal conductivity with increasing burnup,

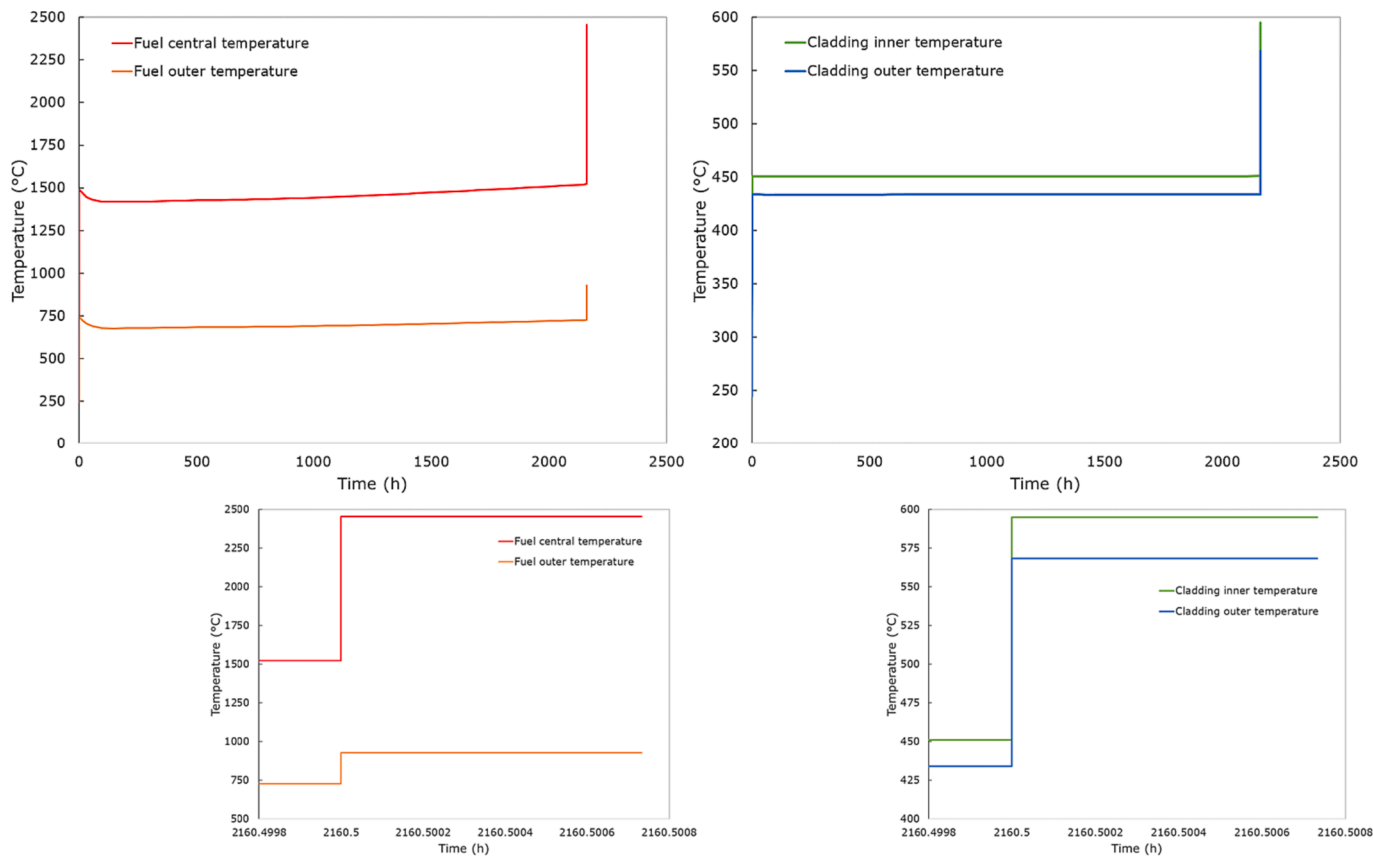


Fig. 2. Top: Evolution of the maximum fuel central and outer temperatures (left, at the peak power node) and of the maximum cladding inner and outer temperatures (right, at the top of fuel column), during the first irradiation cycle and the BPJ at the end of cycle 1 (BPJ1). Bottom: Zoom of the temperature evolutions (left: fuel, right: cladding) during the transient BPJ1 irradiation, before reactor shutdown is performed.

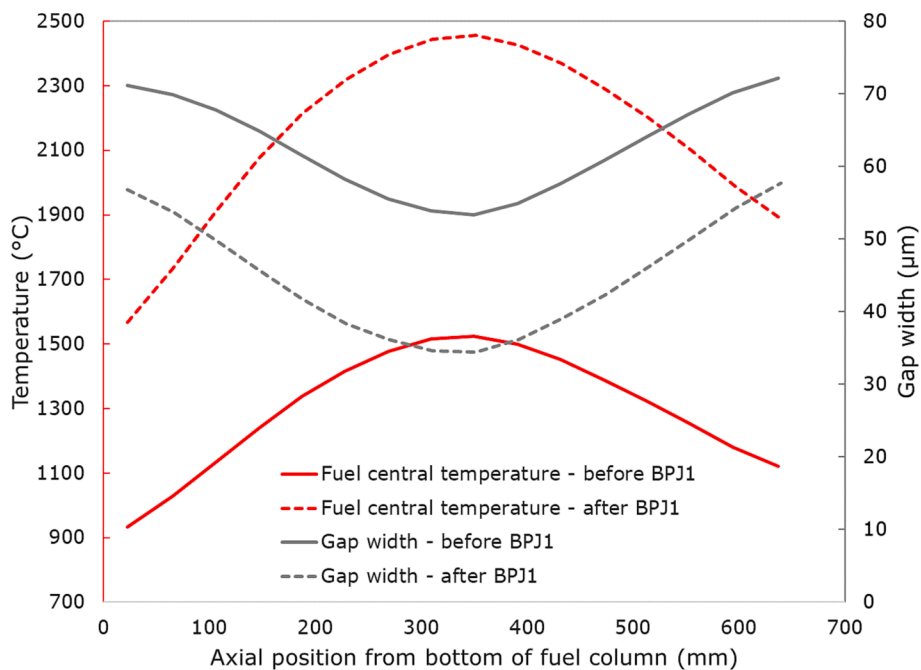


Fig. 3. Axial profiles of the fuel central temperature and fuel-cladding gap width before and after the BPJ1 at the end of cycle 1 (BPJ1).

according to the model employed (Magni et al., 2020, 2021). Nevertheless, the BPJ1 scenario analysed in Section 3.2 is confirmed as the one leading to the highest MYRRHA fuel temperature under operational

transient conditions. Indeed, the peak pin linear power of the hottest pin during normal operation is decreased below 15 kW m^{-1} from cycle 4 on, due to irradiation positions in more peripheral MYRRHA core rings.

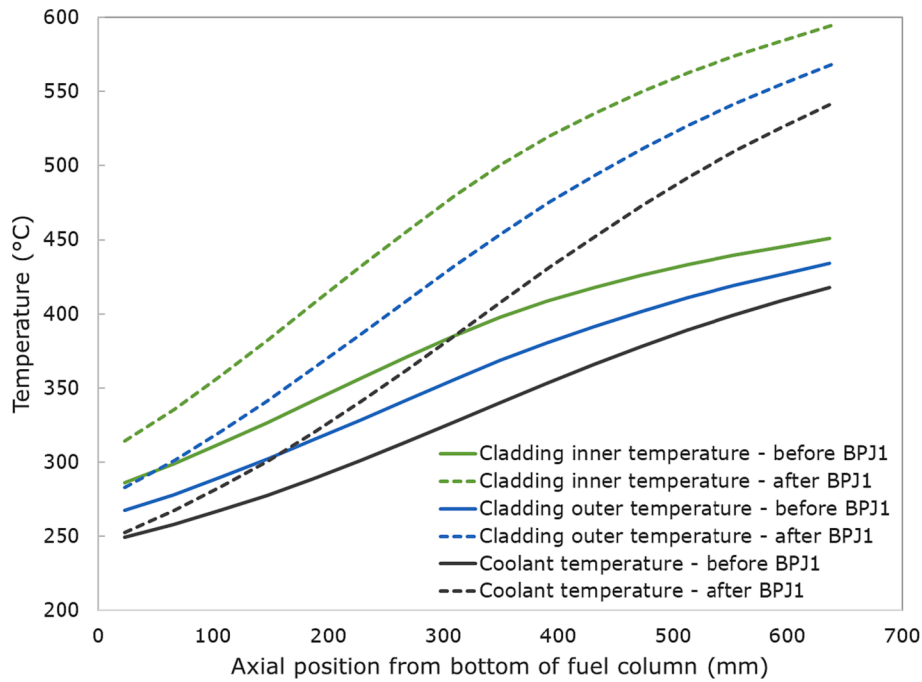


Fig. 4. Axial profiles of cladding inner temperature, cladding outer temperature and coolant bulk temperature, before and after the BPJ at the end of cycle 1 (BPJ1).

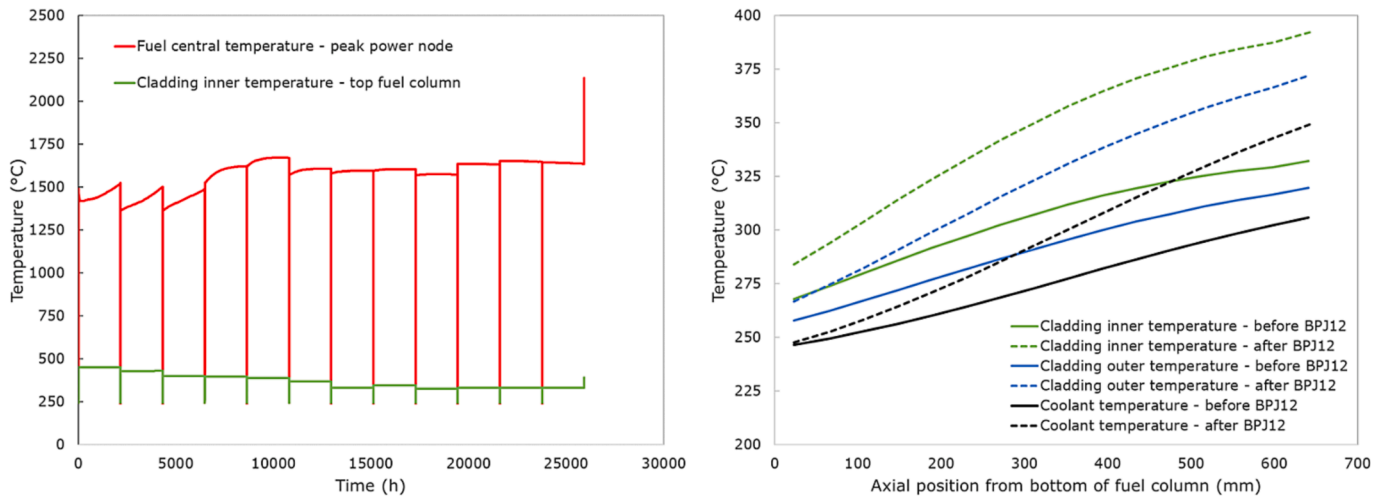


Fig. 5. Left: Evolution of the maximum fuel central temperature (at the peak power node) and cladding inner temperature (at the top of fuel column), during the entire driver fuel irradiation and the BPJ at the end of cycle 12 (BPJ12). Right: Axial profiles of cladding inner temperature, cladding outer temperature and coolant bulk temperature, before and after the BPJ12.

Hence, BPJ transients occurring there lead to a peak linear power below 25.5 kW m^{-1} , while more than 38 kW m^{-1} is reached with BPJ1 when the pin is in the irradiation position closest to the central core spallation target. The linear power level dominates on irradiation effects in determining the maximum fuel temperature reached under operation in the considered MYRRHA design.

Fig. 5 - left also reports the evolution of the cladding inner temperature experienced by the MYRRHA hottest pin during the 12 cycles normal operation before BPJ12 occurs, at the top of fuel column where the cladding is the hottest, extending the result of Fig. 2 - right. From the value during cycle 1 ($\sim 450^\circ\text{C}$), it decreases during irradiation down to $\sim 332^\circ\text{C}$ at cycle 12 being stable during each cycle according to the associated power level. The BPJ12 causes its sudden jump to $\sim 392^\circ\text{C}$. Correspondingly, the cladding outer temperature at the hottest axial location jumps from $\sim 320^\circ\text{C}$ to $\sim 372^\circ\text{C}$, while the bulk coolant

temperature from $\sim 306^\circ\text{C}$ to $\sim 349^\circ\text{C}$. These values are confirmed by the axial profiles of the coolant and cladding temperatures before and after BPJ12, shown by Fig. 5 – right. The thermal conditions of coolant and cladding, relevant in terms of cladding corrosion, are hence of even less concern at the end of the MYRRHA irradiation compared to the beginning of irradiation (cycle 1, Fig. 4).

The evolution of the fuel-cladding gap width is presented in Fig. 6 – left, determined by the differential dynamics of fuel outer and cladding inner radii. TRANSURANUS yields a progressively decreasing gap width up to the fifth cycle of the MYRRHA nominal irradiation,⁴ mainly driven by fuel thermal expansion and temperature- / irradiation-driven

⁴ Sudden increases of the fuel-cladding gap width are predicted during the irradiation inter-cycles, when a batch of fuel pins is moved from the previous to the next irradiation position in the MYRRHA core.

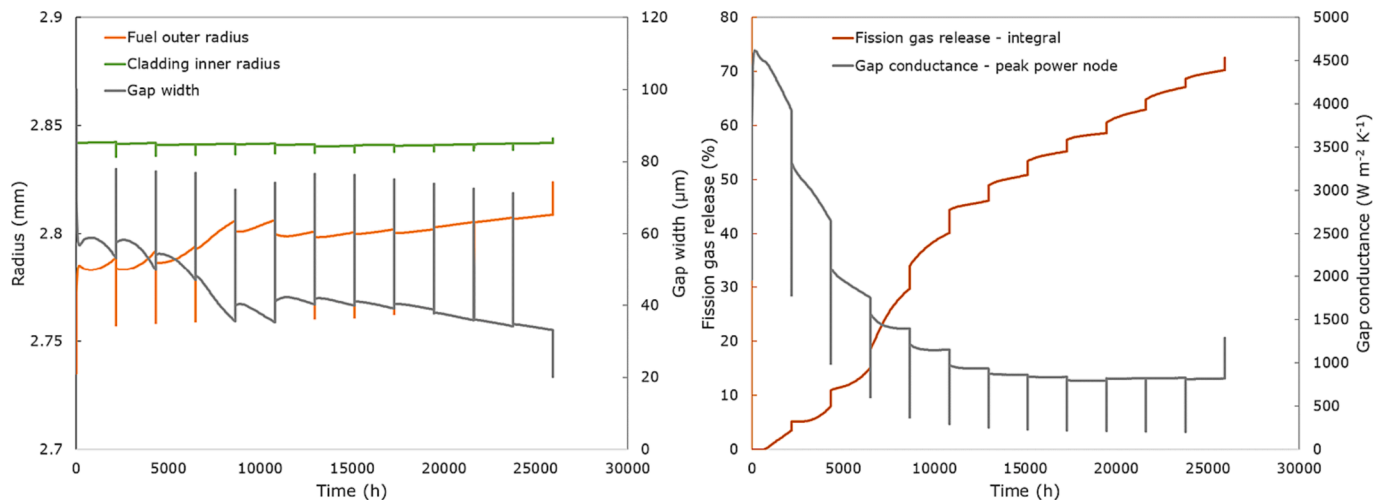


Fig. 6. Evolution of fuel outer radius, cladding inner radius, fuel-cladding gap width at the peak power node (left) and of integral fission gas release and gap conductance at the peak power node (right) during the entire driver fuel irradiation and the BPJ at the end of cycle 12 (BPJ12).

deformations (e.g., swelling) of both fuel pellets and cladding.⁵ Then, this evolution trend of the residual gap width is compensated by a simultaneous high rate of fission gas release (Fig. 6 – right) which limits the fuel swelling coherently calculated via the SCIANTIX physics-based approach. The fuel micro-cracking model implemented in SCIANTIX, causing burst releases of gas from the grain boundaries of the fuel ceramic material opened during power (and temperature) transients,⁶ is responsible for the stepwise increase of the FGR up to almost 75% at the end of irradiation. The FGR proves to have the dominant impact on the gap conductance degradation up to the end of cycle 12, while the occurrence of BPJ12 causes a step-increase of the gap conductance linked with the sudden decrease of the gap size due to the thermal expansion of the hotter fuel during the fast transient. As shown by both Fig. 6 – left and Fig. 7, the gap never reaches closure during the MYRRHA driver fuel irradiation (similarly to the *reference* calculation performed in Magni et al. (2022)) and not even after the final BPJ12. A residual gap size of minimum $\sim 20 \mu\text{m}$ is yielded after the BPJ12, from a gap of $\sim 33 \mu\text{m}$ before BPJ12.⁷

⁵ Fuel relocation also contributes to the evolution of the fuel-cladding residual gap width, under transient conditions and especially at beginning of irradiation, e.g., during the first rise to power that already causes fuel cracking and the consequent displacement of the fuel fragments, inducing an increase in the pellet diameter (Oguma, 1983). Hence, together with the mentioned fuel deformation mechanisms under irradiation (thermal expansion, swelling, creep), relocation impacts on the predicted gap conductance via the gap size, influencing in turn the calculated fuel temperature. In general, fuel relocation depends on the irradiation conditions (linear power level above the threshold for fuel cracking) and on the fuel burnup level. A model suitable for fast reactor conditions is available in TRANSURANUS (European Commission, 2022; Preusser and Lassmann, 1983; Lassmann and Hohlefeld, 1987) and employed for the present simulations, although relocation is a phenomenon stochastic in nature and despite the associated modelling uncertainties (which is reflected by the different modelling approaches adopted by different fuel performance codes, as discussed in Luzzi et al. (2023, 2021)). The uncertainty on the extent of fuel relocation can play a role in predicting the occurrence of fuel-cladding mechanical interaction, although this is still not expected in the MYRRHA pins considering the residual open gap even after BPJ12 ($\sim 20 \mu\text{m}$, Fig. 6 - left).

⁶ The SCIANTIX model for the micro-cracking of the fuel grain boundaries is described in Pizzocri et al. (2020) and already assessed/applied to fast reactor irradiation conditions in Luzzi et al. (2023), Magni et al. (2022).

⁷ The residual gap at the end of cycle 12 calculated here is wider than $\sim 10 \mu\text{m}$ obtained in Magni et al. (2022). The present results is due to a reduced fuel swelling linked to the higher fission gas release at extended burnup provided by the fuel micro-cracking model.

Finally, despite the fact that the occurrence of the BPJ12 transient causes a sudden increase of the stress levels in the cladding calculated by TRANSURANUS, the equivalent Von Mises stress values remain low and far from any concern related to cladding plasticity or integrity (by comparison with the DIN 1.4970 yield stress as a function of temperature, Section 4). The highest Von Mises stress in the cladding (radially averaged) actually occurs at the beginning of cycle 1 of the MYRRHA normal operation, equal to $\sim 32 \text{ MPa}$ at the peak power node, while the value reached with the BPJ12 is $\sim 20 \text{ MPa}$. The occurrence of a BPJ at the beginning of cycle 1, when the cladding equivalent stress is the highest, would cause its jump to $\sim 50 \text{ MPa}$ (again, averaged at the peak power node). For what concerns local stress values, the maximum Von Mises stress after BPJ12 is $\sim 35 \text{ MPa}$ at the cladding outer radius at the peak power node, while it would reach $\sim 110 \text{ MPa}$ after a BPJ at the beginning of cycle 1, at the cladding inner radius at the peak power node. The latter is the highest equivalent stress locally experienced by the cladding during any operative condition (both nominal and transient) of the MYRRHA driver pins, according to the best-estimate TRANSURANUS calculations performed. The absence of gap closure and consequently of fuel-cladding contact pressure helps in limiting the stress state inside the DIN 1.4970 cladding material. This outcome is in line with the analysis of the MYRRHA cladding stress during normal operation already performed in Magni et al. (2022).

4. Compliance with design limits

The fuel performance results presented and discussed in Section 3 must be compared with design limit values for relevant thermal–mechanical quantities, to assess the safety of MYRRHA driver fuel pins even under potential operational transient conditions. Table 1 summarizes the TRANSURANUS predictions against the main design limits adopted in this work (Section 2.2), in case of both over-power BPJ transients of concern for MYRRHA considered.

The beam power jump occurring at the end of irradiation cycle 1 (BPJ1) corresponds to the transient scenario of most concern for the maximum fuel temperature, considering the corresponding highest pin linear power during the MYRRHA driver operation. Indeed, the minimum margin to fuel melting is reached according to TRANSURANUS calculations, at the axial peak power node of the hottest pin, still of $\sim 145^\circ\text{C}$ with respect to the design limit preventing fuel melting issues. It must be noted, however, that this design limit is conservatively set at 2600°C , but the fuel melting (solidus) temperature is actually higher (of $\sim 100^\circ\text{C}$, i.e., a realistic value is $\sim 2700^\circ\text{C}$ (Magni et al., 2020)) even accounting for the 30% Pu content in the as-fabricated MYRRHA MOX

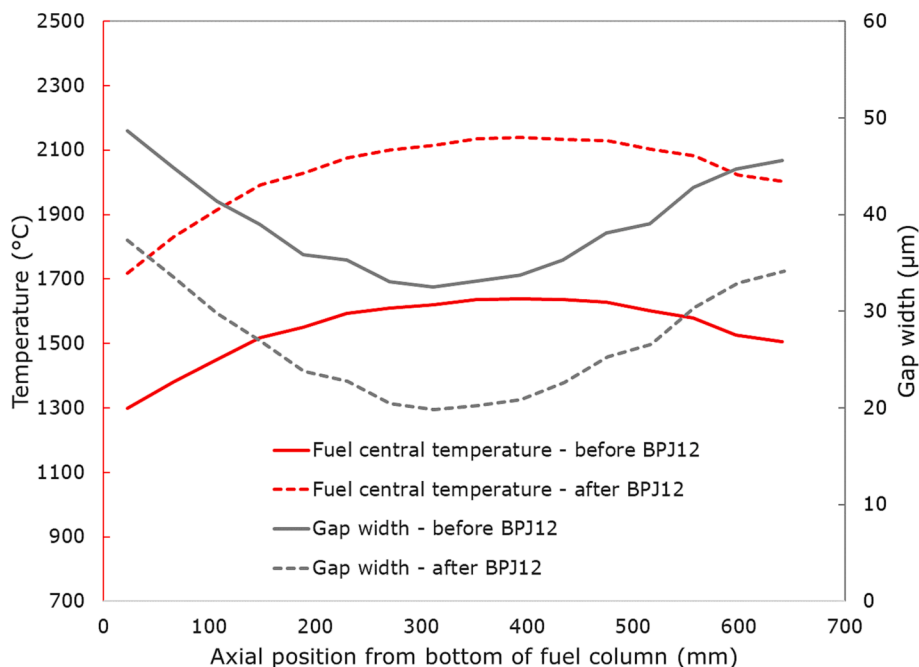


Fig. 7. Axial profiles of the fuel central temperature and fuel-cladding gap width before and after the BPJ at the end of cycle 12 (BPJ12).

Table 1

Maximum fuel temperature and cladding plastic strain calculated by TRANSURANUS during the driver fuel operation of MYRRHA accounting for the BPJ1 and BPJ12 scenarios. The design limits assumed (Magni et al., 2022) are recalled for a direct comparison.

Quantity	Maximum value – BPJ1 scenario	Maximum value – BPJ12 scenario	Adopted design limit
Peak fuel temperature	2455°C (after BPJ1)	2135°C (after BPJ12)	2600 °C
Cladding equivalent plastic strain	0	0	0.5%

fuel and for the final burnup of about 75 Gwd t_{HM}^{-1} at the end of irradiation according to the designed reactor operation. Hence, no pin failure related to fuel melting is foreseen in the case of any BPJ transient occurring during MYRRHA irradiation.

For what concerns the cladding thermal behaviour, the BPJ1 leads to cladding inner and outer maximum temperatures of ~ 595°C and 568°C, respectively. Despite these cladding temperatures, any risk of cladding inner corrosion is avoided due to the absence of fuel-cladding interaction (gap still open), and also no concerns arise due to cladding outer corrosion by the LBE coolant flow, since the transient duration is limited by design to just 3 seconds. The tolerance time of 3 seconds under BPJ conditions before the MYRRHA accelerator shut-off and reactor scram effectively hinders the action of corrosion, occurring on longer time scales. Risks related to the thermal behaviour of the MYRRHA fuel or cladding are even more prevented in the case of the BPJ at the end of irradiation (BPJ12), since the maximum temperatures reached are lower than during BPJ1 (both inner and outer cladding temperatures remain lower than 400°C), due to the lower nominal reactor power. Wider safety margins are hence respected, although this BPJ still causes the fuel and cladding temperatures to increase sharply.

The beam power jump occurring at the end of irradiation (BPJ12) is in principle the most critical scenario in terms of fuel-cladding mechanical interaction and cladding integrity, since this BPJ occurs when the residual gap width is the lowest due to thermal and irradiation-driven fuel deformations prevailing on the cladding dynamics. This situation could lead to cladding plasticity especially in case of gap closure, hence due to the contact pressure exerted by the fuel pellets on the cladding inner surface. Despite this, TRANSURANUS never predicts gap closure even considering both the BPJ transients analysed here,

hence no fuel-cladding interaction occurs during any MYRRHA irradiation condition. As a consequence of this and of a limited gap pressure (maximum 2.9 MPa after BPJ12), during both BPJ1 and BPJ12 the cladding stress levels (in terms of equivalent Von Mises stress) are still limited to tens of MPa as during normal operation (Magni et al., 2022). A conservative (underestimated) value for the yield stress of DIN 1.4970 coherent with the MYRRHA BPJ conditions is estimated as ~ 400 MPa at the highest cladding temperatures reached with the BPJ1, based on (Holmstrom et al., 2017; Strafella et al., 2017, 2017; Weir et al., 1968; Nakatsuka, 1991; Luzzi et al., 2014) and accounting for the cold-working of the steel (Magni et al., 2022). This value accounts for the worst cladding temperature and also for MYRRHA irradiation effects on the cladding yielding behaviour. Values of equivalent stress of tens of MPa imply that the MYRRHA cladding mechanical performance is in the elastic regime during any operative condition and cladding plasticity is avoided.

Hence, it can be concluded that the compliance of the MYRRHA driver pin performance with design limits is satisfactory even under operational transient scenarios triggered by the coupling of the reactor with the MYRRHA accelerator, guaranteeing the pin safety under any possible irradiation condition (nominal and over-power) within the sub-critical core. This is even more true considering that the performance of the hottest pin (experiencing the worst irradiation conditions in terms of linear power, neutron fluxes and coolant temperature) is evaluated in the present analysis, against conservative safety criteria. This approach is selected on purpose to provide conservative indications useful for the development of the MYRRHA reactor, whose design shows a remarkably high safety.

5. Conclusions and further developments

This work consists of the first safety assessment of MYRRHA “Revision 1.6” driver fuel pins under operational over-power (Beam Power Jump) transient scenarios triggered by the external accelerator coupled to the sub-critical reactor core. This represents a complement to the analysis of the MYRRHA normal operating conditions already achieved in Magni et al. (2022). The simulations are performed with the TRANSURANUS fuel performance code, equipped with dedicated models for the mechanical behaviour of the specific MYRRHA cladding (DIN 1.4970) and with comprehensive, physically-grounded correlations for thermal–mechanical properties (thermal conductivity, melting temperature, thermal expansion, Young’s modulus) of the MOX fuel used as a driver fuel in the MYRRHA design considered here. Moreover, the coupling of TRANSURANUS with SCIANITX as a fission gas behaviour module, enabling a physics-based, coherent calculation of gas release and fuel gaseous swelling, is herein applied. The effectiveness of these modelling advancements is demonstrated by their application to the integral pin performance analysis under MYRRHA irradiation scenarios. The level of separate-effect validation of the models (documented in literature) and their mechanistic nature ensure that the outcomes of this work can be deemed as the best-estimate ones at the state of the art concerning the MYRRHA pin performance under reactor operative conditions.

For conservative evaluations, the thermal–mechanical behaviour of the hottest fuel pin in the MYRRHA core (i.e., experiencing the hottest conditions in every irradiation position during the 12-cycles driver operation) is compared with main design limits currently adopted for MYRRHA. The occurrence of BPJ transients at the beginning and at the end of irradiation is analysed, since these BPJs are identified as the most critical for the fuel temperature and for the potential cladding plasticity due to eventual fuel-cladding mechanical interaction, respectively. The simulation outcomes reveal a comfortable safety of driver fuel pins designed for MYRRHA even in over-power transient conditions. Indeed, satisfactory safety margins from limiting values are still respected, indicating the suitability of the U-Pu MOX-fuelled pin design under any irradiation scenario. No concerns related to fuel melting or cladding plasticity / integrity emerge from the advanced TRANSURANUS simulations performed. The results presented in this paper provide first indications supporting the design development of the MYRRHA reactor concept, besides further demonstrating the state-of-the-art capabilities of the TRANSURANUS fuel performance code on fast reactors and extending its applicative range to operational transients in LBE-cooled systems. Nevertheless, from both the fuel performance code and MYRRHA scenarios points of view, additional needed developments and analyses are identified from this work.

Advancements towards considering the corrosion of the DIN 1.4970 austenitic stainless-steel, selected as cladding for the MYRRHA pins, from the LBE coolant is of sure interest for the optimization of both the core design and irradiation conditions. Although not considered by the present simulations due to the current lack of a specific and reliable model, as discussed in Section 3.1, outer cladding corrosion is a critical issue for the cladding performance since it impacts both the cladding-coolant heat transfer as well as the cladding structural integrity. This represents a general MYRRHA-oriented modelling development, important especially for advanced assessments of the normal operating conditions from which BPJs can develop. A MYRRHA-specific and reliable description of the LBE-DIN 1.4970 corrosion process should benefit from dedicated experimental data currently missing, in support of the modelling activity. Moreover, related to the inner (fuel-side) corrosion of the cladding, more insights on the potential gap closure would come from the proper consideration of fuel relocation and its accommodation. This would impact on the fuel-cladding mechanical interaction and on the cladding stress levels via the contact pressure, leading to improved

evaluations of the safety margins concerning the cladding mechanical behaviour. Linked to the proper modelling of the gap width evolution, additional work should be devoted to the mechanical models for the MYRRHA cladding steel used in this work, e.g., the modelling of irradiation-induced creep which is based on a limited experimental dataset and hence still open for refinements and validation.

Lastly, sensitivity analyses are recognized as a fundamental step to complement the deterministic analyses performed in this work. The calculation results presented here rely on the best-estimate models currently available in the TRANSURANUS fuel performance code coupled to the SCIANITX inert gas behaviour module, for the properties and phenomena of fuel, cladding and LBE coolant, on the basis of a first model sensitivity analysis already performed in Magni et al. (2022) for the normal operation of MYRRHA. Further sensitivity analyses should extend this work and focus on e.g., occurrences of BPJ transients at different irradiation times, the potential normal operation of MYRRHA at increased power, the uncertainty associated to relevant properties as the fuel thermal conductivity or the fuel-cladding gap conductance. This will be explored in follow-up works.

From the MYRRHA system point of view, the critical configuration of the reactor core should be also explored besides the sub-critical one analysed in this work, towards the complete investigation of the possible scenarios. This involves the assessment of the driver (MOX) fuel pin performance under both normal operation and accidental scenarios of concern for a critical core, e.g., Reactivity-Initiated Accidents (RIAs). Finally, advanced fuel designs, specifically minor actinide (Am, Np)-bearing MOX, are currently under consideration aiming at actinide burning and transmutation via fast reactor irradiation. The feasibility of this option in MYRRHA is being studied within the PATRICIA European H2020 Project (European Union, 2020). Hence, the performance under irradiation (both normal and transient operation) of Am-bearing MOX fuel pins in the MYRRHA sub-critical / critical reactor core will be the subject of future assessment studies.

CRedit authorship contribution statement

A. Magni: Conceptualization, Methodology, Software, Investigation, Validation, Data curation, Visualization, Writing – original draft, Writing – review & editing. **M. Di Gennaro:** Visualization, Writing – review & editing. **E. Guizzardi:** Investigation, Software, Validation, Visualization, Writing – review & editing. **D. Pizzocri:** Conceptualization, Methodology, Investigation, Validation, Visualization, Writing – review & editing. **G. Zullo:** Visualization, Writing – review & editing. **L. Luzzi:** Resources, Supervision, Funding acquisition, Project administration, Visualization, Writing – review & editing.

Declaration of Competing Interest

The authors declare that they have no known competing financial interests or personal relationships that could have appeared to influence the work reported in this paper.

Data availability

Data will be made available on request.

Acknowledgments

This work has received funding from the Euratom research and training programme 2014-2018 through the INSPYRE Project under grant agreement No 754329. The authors would like to acknowledge Dr. B. Boer (SCK CEN) for providing the specifications of MYRRHA “Revision 1.6” design and associated irradiation scenarios in the framework of the INSPYRE Project.

References

- Ait Abderrahim, H., et al., 2005. Fuel design for the experimental ADS MYRRHA. In: Technical Meeting on Use of LEU in ADS, 10-12 October 2005. IAEA, Vienna, Austria.
- Ait Abderrahim, H., Baeten, P., De Bruyn, D., Fernandez, R., 2012. MYRRHA - A multi-purpose fast spectrum research reactor. *Energy Convers. Manag.* 63, 4–10.
- Ait Abderrahim, H., Baeten, P., Sneyers, A., Schyns, M., Schuurmans, P., Kochetkov, A., Van den Eynde, G., Biarrotte, J.-L., Garbil, R., Davies, C., Diaconu, D., 2020. Partitioning and transmutation contribution of MYRRHA to an EU strategy for HLW management and main achievements of MYRRHA related FP7 and H2020 projects: MYRTE, MARISA, MAXSIMA, SEARCH, MAX, FREYA, ARCAS. *EPJ Nuclear Sci. Technol.* 6, 33.
- Ait Abderrahim, H., De Bruyn, D., Dierckx, M., Fernandez, R., Popescu, L., Schyns, M., Stankovskiy, A., Van den Eynde, G., Vandeplassche, D., 2019. MYRRHA accelerator driven system programme: Recent progress and perspectives. *Nucl. Power Eng.* 2019 (2), 29–42.
- De Bruyn, D., Abderrahim, H.A., Baeten, P., Leysen, P., 2015. The MYRRHA ADS project in Belgium enters the Front End Engineering Phase. *Phys. Procedia* 66, 75–84.
- De Bruyn, D., et al., Recent Developments in the Design of the Belgian MYRRHA ADS Facility. In: *2016 International Congress on Advances in Nuclear Power Plants (ICAPP'16)*, 17-20 April 2016, San Francisco, California, USA, 2016.
- Engelen, J., et al., 2015. MYRRHA: Preliminary front-end engineering design. *Int. J. Hydrogen Energy* 40 (44), 15137–15147.
- European Commission, 2022. *TRANSURANUS Handbook*. Joint Research Centre, Karlsruhe, Germany.
- European Union's Horizon 2020 Research and Innovation programme, "PATRICIA - Partitioning And Transmuter Research Initiative in a Collaborative Innovation Action", 2020. [Online]. Available: <https://patricia-h2020.eu/>.
- Fernandez R., et al., The evolution of the primary system design of the MYRRHA facility. In: *FR17 - IAEA International Conference on Fast Reactors and Related Fuel Cycles: Next Generation Nuclear Systems for Sustainable Development*, 26–29 June 2017, Yekaterinburg, Russia, 2017.
- GIF (Generation IV International Forum). GIF R&D Outlook for Generation IV Nuclear Energy Systems - 2018 Update, 2018.
- GIF (Generation IV International Forum). Annual Report 2020, 2020.
- Holmstrom, S., et al., 2017. Determination of High Temperature Material Properties of 15–15Ti steel by Small Specimen Techniques. JRC Report EUR 28746 EN. Publications Office of the European Union, Luxembourg.
- Lassmann, K., 1992. TRANSURANUS: a fuel rod analysis code ready for use. *J. Nucl. Mater.* 188C, 295–302.
- Lassmann, K., Hohlefeld, F., 1987. The revised URGAP model to describe the gap conductance between fuel and cladding. *Nucl. Eng. Des.* 103 (2), 215–221.
- Lemehov, S., 2020. New correlations of thermal expansion and Young's modulus based on existing literature and new data. INSPYRE Deliverable D6.3.
- Locatelli, G., et al., 2013. Generation IV nuclear reactors: Current status and future prospects. *Energy Policy* 61, 1503–1520.
- Luzzi, L., et al., 2014. Modeling and Analysis of Nuclear Fuel Pin Behavior for Innovative Lead Cooled FBR. ENEA Report Rds/PAR2013/022.
- Luzzi, L., et al., 2021. Assessment of three European fuel performance codes against the SUPERFACT-1 fast reactor irradiation experiment. *Nucl. Eng. Technol.* 53, 3367–3378.
- Luzzi, L., Cammi, A., Di Marcello, V., Lorenzi, S., Pizzocri, D., Van Uffelen, P., 2014. Application of the TRANSURANUS code for the fuel pin design process of the ALFRED reactor. *Nucl. Eng. Des.* 277, 173–187.
- Luzzi, L., Barani, T., Boer, B., Del Nevo, A., Lainet, M., Lemehov, S., Magni, A., Marelle, V., Michel, B., Pizzocri, D., Schubert, A., Van Uffelen, P., Bertolus, M., 2023. Assessment of INSPYRE-extended fuel performance codes against the SUPERFACT-1 fast reactor irradiation experiment. *Nucl. Eng. Technol.* 55 (3), 884–894.
- Magni, A., et al., 2020. Modelling and assessment of thermal conductivity and melting behaviour of MOX fuel for fast reactor applications. *J. Nucl. Mater.* 541, 152410.
- Magni, A., et al., 2021. Modelling of thermal conductivity and melting behaviour of minor actinide-MOX fuels and assessment against experimental and molecular dynamics data. *J. Nucl. Mater.* 557, 153312.
- Magni, A., et al., 2022. Application of the SCIANITX fission gas behaviour module to the integral pin performance in sodium fast reactor irradiation conditions. *Nucl. Eng. Technol.* 54, 2395–2407.
- Magni, A., et al., 2022. Extension and application of the TRANSURANUS code to the normal operating conditions of the MYRRHA reactor. *Nucl. Eng. Des.* 386, 111581.
- Magni, A., et al., 2022. Fuel Performance Simulations of ESNII Prototypes: Results on the MYRRHA Case Study. INSPYRE Deliverable D7.5.
- Magni, A., Del Nevo, A., Luzzi, L., Rozzia, D., Adorni, M., Schubert, A., Van Uffelen, P., 2021. The TRANSURANUS fuel performance code. In: *Nuclear Power Plant Design and Analysis Codes*. Elsevier, pp. 161–205. Chap. 8.
- MYRRHA Consortium. MYRRHA Project website. 2022. [Online]. Available: <https://www.myrrha.be/>.
- Nakatsuka, M., 1991. Mechanical properties of neutron irradiated fuel cladding tubes. *J. Nucl. Sci. Technol.* 28 (4), 356–368.
- OECD/NEA, 2015. Handbook on Lead-bismuth Eutectic Alloy and Lead Properties, Materials Compatibility, Thermal-hydraulics and Technologies, 2015 Edition. Technical Report NEA No. 7268.
- Oguma, M., 1983. Cracking and relocation behavior of nuclear fuel pellets during rise to power. *Nucl. Eng. Des.* 76 (1), 35–45.
- Pizzocri, D., et al., 2020. SCIANITX: A new open source multi-scale code for fission gas behaviour modelling designed for nuclear fuel performance codes. *J. Nucl. Mater.* 532, 152042.
- Pizzocri, D. et al., Coupling of SCIANITX and TRANSURANUS: Simulation of integral irradiation experiments focusing on fission gas behaviour in light water reactor conditions. In: *International Workshop Towards Nuclear Fuel Modelling in the Various Reactor Types across Europe*, 28-30 June 2021, online, 2021.
- Preusser, T., Lassmann, K. Current status of the transient integral fuel element performance code URANUS. In: *SMiRT 7*, 22-26 August 1983, Chicago, USA, 1983.
- Romerojo, P., Álvarez-Velarde, F., García-Herranz, N., Serot, O., Chebboubi, A., 2019. Nuclear data analyses for improving the safety of advanced lead-cooled reactors. *EPJ Web Conf.* 211, 05002.
- Romerojo, P. et al., 2017. Neutron-induced nuclear data for the MYRRHA fast spectrum facility. *EPJ Web Conf.*, 146; 09007.
- Schubert, A., et al., Present Status of the MOX Version of the TRANSURANUS Code. In: *EHPG Meeting on High Burn-up Fuel Performance*, 9-14 May 2004, Sandefjord, Norway, 2004.
- SNETP, 2020. Sustainable Nuclear Energy Technology Platform. ESNII - SNETP website [Online]. Available: <https://snetp.eu/esnii/>.
- Strafella, A., Cogliatore, A., Fabbri, P., Salernitano, E., 2017. 15-15Ti(Si) austenitic steel: creep behaviour in hostile environment. *Frat. ed Integrità Strutt.* 11 (42), 352–365.
- Strafella, A., Cogliatore, A., Salernitano, E., 2017. Creep behaviour of 15–15Ti(Si) austenitic steel in air and in liquid lead at 550°C. *Procedia Struct. Integr.* 3, 484–497.
- Toti, A., Vierendeels, J., Belloni, F., 2018. Coupled system thermal-hydraulic/CFD analysis of a protected loss of flow transient in the MYRRHA reactor. *Ann. Nucl. Energy* 118, 199–211.
- Van Den Eynde, G., et al., 2015. An updated core design for the multi-purpose irradiation facility MYRRHA. *J. Nucl. Sci. Technol.* 52 (7–8), 1053–1057.
- Van Uffelen, P., et al., 2020. Incorporation and verification of models and properties in fuel performance codes. INSPYRE Deliverable D7.2.
- Weir, J.R., et al., 1968. Irradiation behavior of cladding and structural materials. Report ORNL-TM-2258.